TES Bolometers With High-Frequency Readout Circuit

Artyom A. Kuzmin, Sergey V. Shitov, Alexander Scheuring, Johannes M. Meckbach, *Member, IEEE*, Konstantin S. Il'in, Stefan Wuensch, *Member, IEEE*, Alexey V. Ustinov, and Michael Siegel, *Member, IEEE*

***Abstract*—In order to improve the frequency-division multiplexing (FDM) in transition edge sensor (TES) imaging arrays, it is suggested to replace commonly used SQUID amplifiers with a semiconductor high-frequency cooled amplifier. This would result in a single 10-GHz bandwidth amplifier serving the array of more than 1000 detectors. The basic idea is to implement an antenna-coupled TES as a load for a high-Q resonator, weakly coupled to a microwave transmission line. This high-frequency scheme substitutes the traditional wire connections to the TES. The NEP as low as 2×10^{-19} W/Hz$^{0.5}$ is estimated at ambient temperature of 300 mK for submicron-size TES absorber made of Ti; the NEP is limited by 3 K noise temperature of the amplifier. To verify the new concept, prototype TES devices made of Nb are developed and tested above 4 K. The NEP of about 1.5×10^{-15} W/Hz$^{0.5}$ is estimated for the experimental micron-size prototype devices made of Nb at 4.5 K. The IV-curves of the TES at different temperatures are recovered using the RF and heat balance models along with the experimental $R(T)$ data; presence of the negative electrothermal feedback is verified.**

***Index Terms*—Bolometer, electrothermal feedback, frequency-division multiplexing (FDM), high-Q resonator, imaging array, terahertz range, transition edge sensor (TES).**

I. Introduction

THE superconducting bolometers based on transition-edge sensing (TES) are nowadays of active interest, due to their great potential for ultra-low-noise operation with noise equivalent power (NEP) down to 10^{-19} W/Hz$^{0.5}$ and below [1]. Usually TES acts as a thermometric device, which changes its resistance abruptly near the temperature of the superconducting transition, thus detecting the power coupled to the attached absorber. This traditional approach unavoidably increases the heated volume/mass over the volume/mass of the thermometer that is limiting sensitivity of the TES-based bolometric device.

The antenna-coupled TES devices are relatively new; they comprise absorber and thermometer in the same physical volume, within a submicron-sized film [2]–[4]. The antenna-coupled TES provides direct dissipation of a time-dependent signal current from the feeding antenna converting it into the Joule heat within the tiny volume of its own electron gas. This "signal heat" is combined with a much larger constant "pre-heat" from the bias current, which sets the temperature within the transition range of the TES. Since the transition region is extremely sensitive, such combining makes a strong time-dependent effect on the TES resistance. Note that the terahertz antenna attached to the TES does not play the role of an absorber, since it does not dissipate any Joule heat; the antenna is assumed as the extension of the lossless optical path providing the energy flow to the absorbing electron gas. The reduction in the volume naturally leads to better sensitivity. However the shorter film results in the lower impedance; 2–3 Ω is typical at the bias point. The low-impedance SQUID sensor is the proven solution in this case.

In order to readout the imaging array, the frequency-division multiplexing method (FDM) [5] has been suggested and tested successfully with practicable systems for more than a few thousand pixels. However, the instantaneous bandwidth of best SQUID-sensors is restricted to few MHz that sets a limit for FDM to less than 1000 channels while the practicable realization contains less than 200 channels [6]. Therefore quite a few SQUIDs are required to serve a large array of detectors. This increases both system complexity and cost and, potentially, limits calibration accuracy/stability due to variations in regimes/parameters of the multiple SQUID readouts. Moreover, the assembly of the low-frequency multiplexing circuit made of lumped elements does not look like an easy procedure.

II. Concept and Approaches

A. General Idea

To improve the capability of the multiplexing circuit for TES arrays by a factor of ∼10 along with using advantages of the integrated circuit (IC) technology, we suggested in [7] to follow the well-known radio engineering approach by going towards higher frequency readout. The usage of microwave IC design opens a variety of ways to build a compact multi-channel FDM system, possibly fully integrated at one wafer with the imaging

Manuscript received July 01, 2012; revised November 19, 2012; accepted December 11, 2012. Date of publication January 28, 2013; date of current version February 07, 2013. This work was supported in part by Russian Foundation for Basic Research under Grant 12-02-01352-a, and by Ministry for Education and Science of Russian Federation under Contract 11.G34.31.0062 and Contract 11.G34.31.0029.

A. A. Kuzmin is with the Moscow Institute of Physics and Technology, 141700, Dolgoprudny, Russia, and also with National University of Science and Technology MISIS, Moscow 119049, Russia(e-mail: artyom.kuzmin@gmail.com).

S. V. Shitov is with V. A. Kotel'nikov Institute of Radioengineering and Electronics, Russian Academy of Sciences, Moscow 125009, Russia and with National University of Science and Technology MISIS, Moscow 119049, Russia (e-mail: sergey3e@gmail.com).

A. Scheuring, J. M. Meckbach, K. S. Il'in, S. Wuensch, and M. Siegel are with Institute of Micro- and Nano-Electronic Systems and DFG-Center for Functional Nanostructures (CFN), Karlsruhe Institute of Technology (KIT), D-76187 Karlsruhe, Germany (e-mail: michael.siegel@kit.edu).

A. V. Ustinov is with Institute of Physics and DFG-Center for Functional Nanostructures (CFN), Karlsruhe Institute of Technology, D-76128 Karlsruhe, Germany and with National University of Science and Technology MISIS, Moscow 119049, Russia (e-mail: alexey.ustinov@kit.edu).

Color versions of one or more of the figures in this paper are available online at http://ieeexplore.ieee.org.

Digital Object Identifier 10.1109/TTHZ.2012.2236148

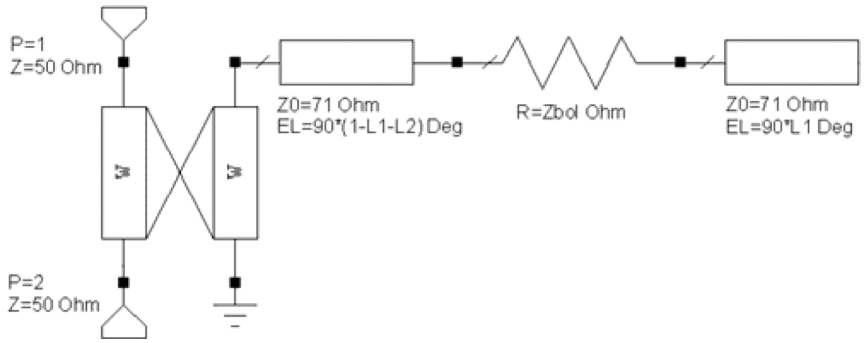

Fig. 1. Equivalent scheme of RF biased TES bolometer. The *open-end* quarter-wave resonator ($Z0 = 71\ \Omega$) is weakly coupled to the throughput line (ports P1 and P2, $Z = 50\ \Omega$). The resonator electrical length (EL) is split in two arbitrary parts $L1$ and $L2 (L1 + L2 \approx 1)$ by the insertion of antenna-coupled TES ($R = Zbol$).

array. The required amplifier can be either a semiconductor cooled wide-band low-noise amplifier (LNA) in the range of about 10 GHz, which can operate at noise temperature in order of 3–4 K [7], or a RF-band SQUID amplifier with noise temperature down to, possibly, 0.1 K [8], [9]. The amplifier match to the detector can be obtained using the standard RF impedance transformation techniques. This would result in a relatively simple system, containing only one amplifier and two coaxial input/output cables, which serve up to 1000 or even more TES detectors. In other words, the low-frequency interconnecting wires and the lumped LC circuits would be replaced with coaxial cables and RF integrated circuits.

B. TES-Loaded Resonant Circuit

It is possible to use the high-Q resonator technology similar to one used for the microwave kinetic inductance detectors (MKID) [11]. We suggest reading the RF response caused by variations in resistivity of the tiny "lumped" TES loading the high-Q quarter-wave resonator. The equivalent scheme of such resonator is shown in Fig. 1. The bias power is applied to the throughput transmission line, which is weakly coupled to a *open-end* quarter-wave resonator. The spectral response of the throughput line contains an absorption/reflection dip, which is the result of the interaction of the incident RF wave with the resonator. It is assumed that the bias current at about 10 GHz pre-heats the TES, providing its resistance within the superconducting transition region at the value about 0.1 $R_{\rm n}$. This pre-heat resistance defines a certain depth in the spectral response of the throughput line corresponding to the dark state of the bolometric device. If the extra heat (current) is applied from the THz antenna, the resistance of the TES will grow, and the Q-factor will change, changing the dip in the throughput spectrum as shown in Fig. 2.

It is important to note here, that such combined heat effect, which is equivalent to the external Joule heat, can be expected, if the thermal relaxation time of the TES film is much longer than the period of the RF current, i.e., the TES must be slow enough. To emphasize the effect of THz heating, the impedance of the antenna has to be well coupled to the impedance of TES driven by RF current. At the same time, the THz signal must not leak away from the antenna to the RF resonator. This can be achieved by using the standard technique of reactive stop-band filters, which must be a part of the RF resonator.

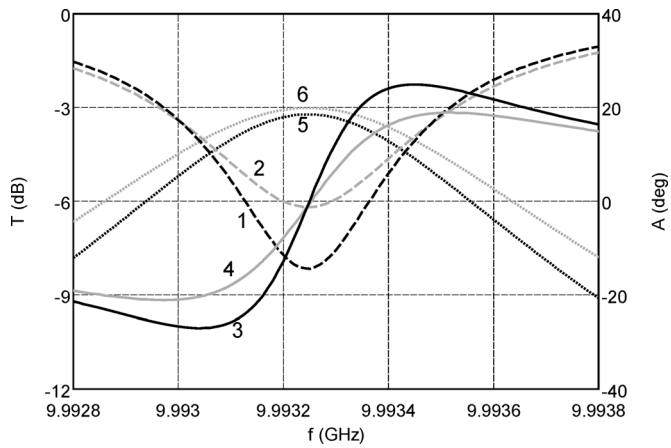

Fig. 2. Calculated *example* of possible Joule heat effect on RF resonator ($Q \approx 10^4$) combined with a general resistance temperature detector (RTD), R, as from Fig. 1. The resistance R grows from 3 Ω to 6 Ω, and the Q-factor changes approximately 25%, thus varying the RF throughput signal (1) to about 2 dB (2). Numbers denote: (3) and (4) are variation in phase, (5) and (6) are power transfer to RTD.

To understand whether it is possible to design a high-Q resonator loaded with a desired resistor, the embedding (source) impedance, $Zemb$, over the sensor, $Zbol$, is calculated for the resonator from Fig. 1. The graph presented in Fig. 3 sets the relation between the source impedance and the optimum position for the insertion; each value corresponds to the same Q-factor $Q \approx 10^4$ at 10 GHz. Note that the small THz-antenna circuit is assumed to be a lumped part of the resonator, so it is not shown in Fig. 1.

The general scheme of a possible imaging array is presented in Fig. 4. Note that all N resonators ($N = 5$ in this example) are spatially distributed over the image aperture and tuned to slightly different frequencies fitting to the comb spectrum of the RF bias. The THz signal illuminating the array provides the extra Joule heat for each pixel and changes their Q-factors independently (changes the dips as in Fig. 2). The analysis of components of the output comb signal will reveal the brightness of the THz image at relevant pixels.

The new approach might bring a few advantages over both "traditional" MKID and TES. i) Since the TES behave as a lumped resistor (1 Ω and up), it is definitely possible to match to the receiving antenna, much easier than MKID. ii) The response

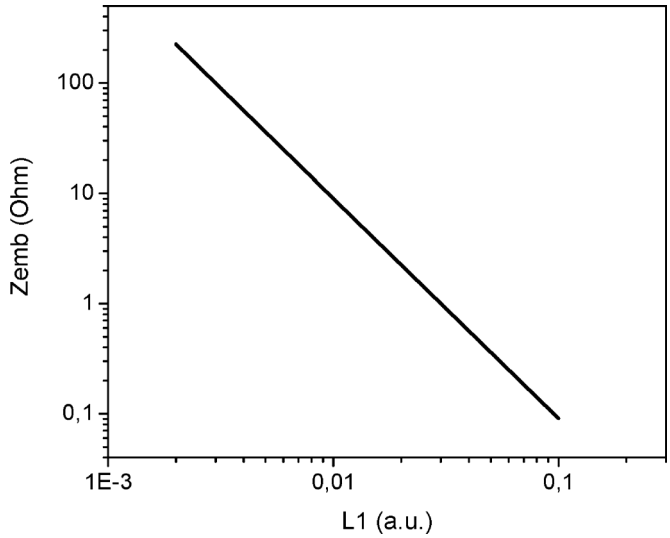

Fig. 3. Calculated embedding (source) impedance for a TES inserted in the resonator ($Q \approx 10^4$) as a function of arbitrary position, $L1$, from Fig. 1. Note the wide range of possible values for the matched resistance of TES.

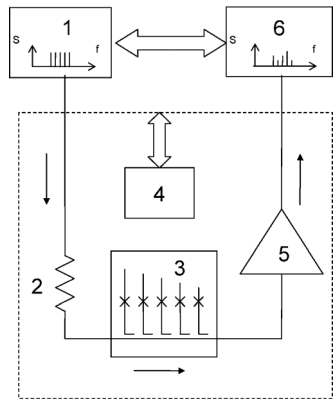

Fig. 4. Conceptual scheme of the imaging receiver. 1—Reference comb generator. 2—Cold attenuator for cutting 300-K thermal noise. 3—Chip with TES-loaded resonators coupled to common throughput line. 4—Refrigerator and controller providing stable temperature for the bath, $T_{\rm bath}$ (dashed). 5—low-noise amplifier LNA. 6—Registering and spectrum/amplitude analyzing device.

of TES is generally independent on frequency, since the only Joule heat effect is detected. iii) In respect to present (published) TES technology, the *open-end* high-Q resonator will provide almost perfect protection of the nanometer-scale TES from electrical shocks including static discharge; there is no wire chain connected to the TES and the effective capacitance of the RF interface is extremely small. The video-bandwidth of the detector is limited to the bandwidth of the resonator that is about 500 kHz in our case.

C. Design Approach and Estimate for NEP

The prototype detector circuit for the temperature 280–300 mK is developed on the base of a coplanar waveguide (CPW) following the conceptual scheme from Fig. 1. All parts of the circuit can be fabricated of thick (200–300 nm) films of Niobium (Nb) on either silicon or sapphire substrates. The TES can be made of thin (20–30 nm) films of Titanium (Ti, $T_{\rm c}$ about 300 mK), which demonstrates the pronounced effect of electron gas heating at this temperature [4]. A compact THz-range double-slot antenna [12] integrated with the TES has to be placed in the CPW resonator according to the data from Fig. 3 and then positioned in a focus of a hyper-hemispherical lens, which provides the Gaussian beam waist on top of the antenna.

We have performed the detailed EM simulation of this prototype detector circuit using the parameters from Fig. 1. It should be noted here that adding the antenna results in a RF discontinuity and noticeably modifies the resonator. Therefore the accurate iterated numerical simulations are required for finding the proper embedding impedance, thus making the Fig. 3 an important but rather qualitative illustration.

We have estimated the sensitivity of the new device via the virtual (numerical) experiment using the particular EM-layout as described below. First, we analytically approximated the superconducting transition $R(T)$ using the following formula:

$$R(T) = R_{\rm n}\left[\exp\left(-\frac{4(T-T_{\rm c})}{\Delta T_{\rm c}}\right)+1\right]^{-1}. \qquad (1)$$

The normal resistance just above $T_{\rm c} \approx 300$ mK is $R_{\rm n} \approx 50\ \Omega$; it is reported $\Delta T_{\rm c} = 2$ mK for a good example of Ti film.

At the second step we set the bias point for the TES at $4.5\ \Omega \approx 0.1R_{\rm n} = R_{\rm n1}$. To calculate the response of the throughput RF line, we use a small probe signal, which is assumed to provide small (20%) growth of the TES resistance to $R_{\rm n2} = 5.5\ \Omega$. This ensures that TES operates within the region of its linear response. Solving (1) for T we get two electron gas temperatures: $T_{\rm e1} = 298.843$ mK and $T_{\rm e2} = 298.955$ mK.

The second step includes Joule heat balance. This allows for finding the bias power, which corresponds to $T_{\rm e1}$ and its *combination* with the probe signal yielding $T_{\rm e2}$. The volume, ν, of a practicable TES absorber can be set for 1 μm $\times$ 200 nm $\times$ 20 nm. Suggesting the Andreev mirrors [13] present at the Ti/Nb interface, we can use the heat balance equation for the power $P_{\rm J}$ absorbed by TES from the resonator [14],

$$P_{\rm J}(T_{\rm e}) = \nu\Sigma\left(T_{\rm e}^5 - T_{\rm bath}^5\right). \qquad (2)$$

Here $\Sigma = 3\times10^{-9}$ W/(μm^3 K^5) is the material parameter of Ti, $T_{\rm bath} = 280$ mK—phonon temperature defined by the refrigerator (by the bath), $T_{\rm e}$—electron gas temperature due to the *combined* RF power. The power of the bias and the probe signals can be calculated from (2) as $P_{\rm J}(T_{\rm e1}) = 7.95\ 10^{-15}$ W and $P_{\rm SIG} = P_{\rm J}(T_{\rm e2}) - P_{\rm J}(T_{\rm e1}) = 0.053\ 10^{-15}$ W respectively. Using the linear EM-model of the circuit from Fig. 1 we obtain S-parameters at the resonance frequency: the dip $S_{21} = -0,69$ dB and the variation $\Delta S_{21} = -0,07$ dB ($\approx$ 1.3%). The element *Zbol* is replaced in the simulation with the port P3. The transfer of the bias power from the throughput line to the TES is $S_{31} = -11.4$ dB ($\approx$7%). Using S_{31} we get for the throughput line $P_{\rm BIAS} = P_{\rm J}(T_{\rm e1})/S_{31} = 1,09\ 10^{-13}$ W and for its variation caused by the extra probe signal $\Delta P_{\rm BIAS} = P_{\rm BIAS} \times \Delta S_{21} = 1.42\ 10^{-15}$ W. The incremental voltage, $\Delta U_{\rm BIAS}$, *in the throughput* transmission line ($Z_0 = 50\ \Omega$Ohm) can be calculated as

$$\Delta U_{\rm BIAS} = \frac{\Delta P_{\rm BIAS} Z_0}{2\sqrt{P_{\rm BIAS} Z_0}}. \qquad (3)$$

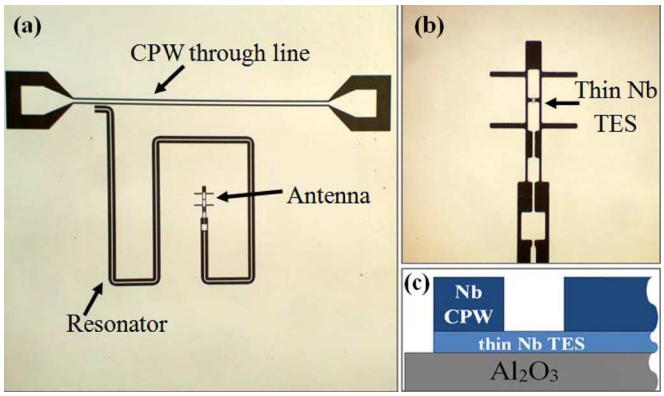

Fig. 5. (a) Optical photo of experimental chip with quarter-wave resonator at about 6 GHz incorporating a double-slot THz antenna. (b) Close-up of 600-GHz double-slot antenna with $5 \times 2.5 \times 0.015$ μm^3 Nb TES. (c) Schematic side view of Nb double layer structure on sapphire substrate.

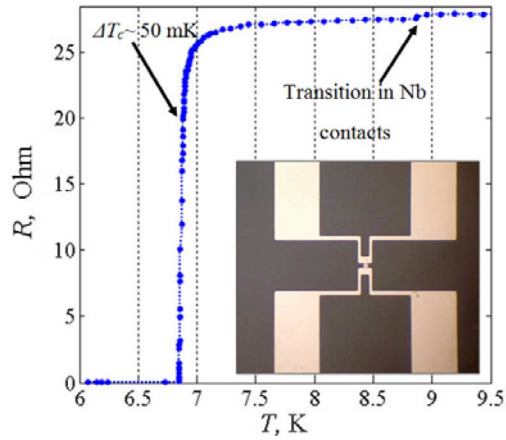

Fig. 6. Superconducting transition curve $R(T)$ of the Nb witness bridge (the insert image) near its critical temperature. The film thickness is about 15 nm. The witness bridge was fabricated on the same wafer having the same size as the TES in resonator from Fig. 5.

Note that the response $\Delta U_{\rm BIAS}$ is the *incremental* voltage at the input of the LNA, and the response is growing with increase of the bias power. Using (3) we can calculate power-to-voltage responsivity $S = \Delta U_{\rm BIAS}/P_{\rm SIG} = 2.85 \times 10^8$ V/W at the input of the LNA. Setting the noise temperature of the cooled LNA to $T_{\rm N} = 3$ K, which definitely dominates the noise of the 300-mK device, we calculate the 1-Hz bandwidth voltage noise of LNA as $U_{\rm n} = 4.6 \times 10^{-11}$ V/Hz$^{1/2}$. The estimate for the whole detector-amplifier chain gives $NEP = U_{\rm n}/S = 1.6 \times 10^{-19}$ W/Hz$^{1/2}$, which can be certainly improved for at least one order would a lower noise amplifier be available.

III. Experimental Details and Discussion

A. Fabrication

Since the low-temperature experiments are quite laborious, expensive and time consuming, we decided first to verify our EM-model and most basic approaches at 4-K temperature level. A pilot 4-K device was designed with the resonator from Niobium (Nb) film and TES from Tantalum (Ta) film on c-axis sapphire substrate. However, in the first implementation described below, the Nb process was used for the whole device. Thick (300 nm) Nb with $T_{\rm c} = 8.8$ K was used for the throughput line and for the quarter-wave resonator. To reduce the transition temperature of TES of Nb from 8.8 K to about $T_{\rm c} = 5.5$ K, the intrinsic proximity effect, i.e., decrease of $T_{\rm c}$ with thickness of ultra-thin film with $d \leq \xi_0$, was studied by measuring the superconducting transition in test films of different thickness in the range 5–30 nm. The Nb films are sputtered in the UNIVEX 450 magnetron sputtering system at the deposition rate 0.27 nm/s. The process is optimized for the argon gas pressure: films of the best quality (highest $T_{\rm c}$ and RRR) are deposited at 5×10^{-3} mbar. The superconducting and transport properties of the test films are measured with the DC-insert in the transport He^4 Dewar vessel without special temperature stabilization.

The geometry of the pilot device presented in Fig. 5 was formed by the standard optical contact photolithography. At the first step thin (15 nm) Niobium film is deposited on the whole sapphire substrate. At the second step the throughput line, the CPW resonator and the planar antenna are patterned from a thick (200 nm) Niobium film by the lift-off process. Because of *ex situ* process, the cleaning step with the argon gun prior the deposition is performed in order to have a good electrical contact with the TES layer. Finally, the TES bridge of size $5 \times 2.5 \times 0.015$ μm^3 is formed by the Ar^+ ion gun, etching away the bottom layer, using the resist layer and the thick structure of Nb as a mask.

B. DC Measurement

Since the small TES is completely *decoupled* at DC, the direct measurements of its superconducting and thermal properties are not possible. Their estimate is done using a witness structures of the same size and fabricated on the same wafer as the resonators. The critical temperature $T_{\rm c} = 6.7$ K and the transition width $\Delta T_{\rm c} = 50$ mK are measured for the optimized witness bridges as shown in Fig. 6. The transition of thick Nb film is also seen in Fig. 6 at $T_{\rm c} = 8.8$ K. The critical and the hysteretic return currents, $I_{\rm c}$ and I_H, are obtained from the experimental I–V-curves ($T_{\rm bath} = 4.2$ K) in both the liquid He^4 and the He^4 vapor. These currents of the witness bridges are about $I_{\rm c} \approx 4$ mA and $I_{\rm H} \approx 0.5$ mA. Using the value of the hysteresis current in the He^4 vapor one may estimate the thermal conduction coefficient, $G_{\rm th}$. Following [16], we use the power balance equation:

$$P_{\rm J} = I_{\rm H}^2 \cdot R_{\rm N} \approx G_{\rm th}(T_{\rm c} - T_{\rm bath}). \tag{4}$$

Here $R_{\rm N} = 27\ \Omega$ is the normal state resistance of the witness bridge. The estimate for $G_{\rm th}$ is about 4×10^{-6} W/K.

According to the papers [17] and [18], [19] the heat transfer from electrons to phonons in thin films of Nb at about 4 K is of different power than in the formula (2), which is valid for Ti thin films at about 300 mK [4]. For this reason we use the following formula:

$$P_{\rm J} = \nu\Sigma\left(T_{\rm e}^4 - T_{\rm ph}^4\right). \tag{5}$$

Here the material parameter $\Sigma = 8.2 \times 10^{-9}$ W/(μm$^3 \times$ K^4) for Niobium, the volume of the TES absorber is set to $\nu = 5 \times 2.5 \times 0.015$ μm^3. The NEP $= 1.5 \times 10^{-15}$ W/Hz$^{1/2}$ can

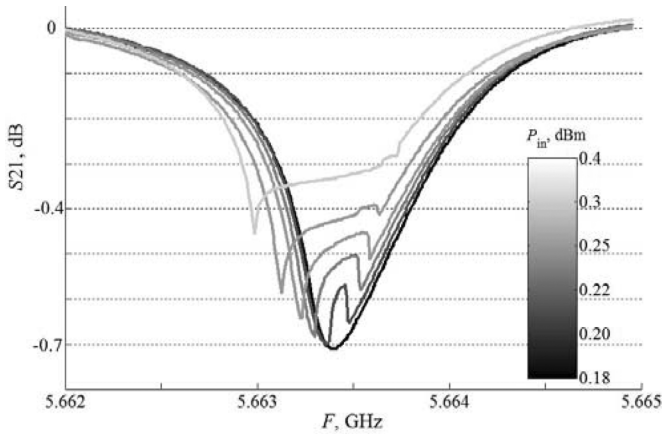

Fig. 7. Frequency dependent transmission of the experimental device at bath temperature about 5 K. The pronounced triggering effect, possibly, to the hot-spot regime occurs around the resonance frequency, i.e., at maximum current in the resonator. The two lowest curves correspond to superconducting state of the resonator; its Q-factor can be estimated as $Q = 7000$.

be estimated using the method described above for the experimental prototype devices made of Nb at 4.5 K.

The estimate for time constant of the thermometer gives $\tau = C/G_{\rm th} \approx 0.5$ ns, where C is calculated from the material parameters as in [17] that is in good agreement with the value of Nb HEBs [18]. Accounting for the value of τ, one may suggest the experimental study at the bias frequencies higher than 4 GHz. At these frequencies the RF bias acts as the Joule heat source, so the resistance of the TES cannot follow the phase of the high-frequency bias current.

C. RF Measurements

The goal of the first experimental run is validation of the RF design at 4-K temperature range. The chip from Fig. 5(a) was mounted on the flat surface of the hyper hemispherical sapphire lens using the cyanoacrylate adhesive. The contact pads of the throughput line are wire-bonded to a printed circuit board (PCB), which serves as the electrical interface between the chip and the input/output SMA-type connectors. The above assembly is mounted to a stick insert, which dips into a vessel with liquid Helium. The temperature range of the experiment was above 4.5 K, since the sample was operated in the dense vapor above the surface of liquid Helium. To obtain the frequency responses, the Agilent PNA-X series network analyzer was used at incident powers ranging from -27 dBm up to $+6$ dBm.

It was initially suggested that the bias point can be set via variation of the incident RF power, which heats the TES to a desired temperature. However we did not find this way productive. The experimental trigger-like response of the device is presented in Fig. 7; it looks as an abrupt deviation from the smooth curve upwards at its very dip. At lower powers (0.2 dBm) the deviation looks as a peak which transforms into two-horn structure at higher powers. The response is very pronounced and demonstrates a clear threshold. We think this is a hot-spot response, since the estimated amplitude of the switching RF current is about the critical current measured at DC for the witness TES. The shape of the resonance curve did not change below the power range presented in the inset for Fig. 7, so we conclude that TES remains in the superconducting state at the lower powers. The Q-factor of about 7000 can be estimated from Fig. 7, along with both the dip and the resonant frequency close to their design values of -0.8 dB and 5.85 GHz, respectively. These data have validated the RF design successfully.

D. Discussion on Regime of Operation

To find the right procedure for biasing the new TES device in linear regime that exclude the trigger-like hot-spot phenomenon, the dynamic model of the system is developed along with the procedure for extraction of I–V-curve at RF (will be published elsewhere). The dynamic model exploits S-parameters of the structure along with physical parameters of the absorber, including $R(T)$. It was found that the dynamic model can explain the major behavior of the experimental device.

To make sure that the stable regime of operation is possible, we have analyzed the S-parameter dependence on R and found the merit of stability, which is related to ratio $R/R_{\rm emb}$ of the resistance of the TES at its bias point, R, and the embedding impedance of the resonator at its resonance, $R_{\rm emb}$. For the case of $R/R_{\rm emb} < 1$ the operation is unstable, since the resonator acts as a current source, which gains the electrical power at the resistor once its resistance starts increasing due to whatever reasons; here we got the *positive* electrothermal feedback. This is exactly what we can see in the experiment (see Fig. 7)—fast triggering from zero resistivity to the normal state—the hot-spot nucleation in the middle of the dip. In the case of $R/R_{\rm emb} > 1$ the resonator acts as a voltage source, which supports the decrease of the electrical power, while the resistance of the TES is growing. Here we got the *negative* electrothermal feedback.

Following the dynamics model, it is suggested to set the operation regime in the following way. First we fix the bath temperature, $T_{\rm bath}$, and set the RF power to the level which corresponds to $P_{\rm J}$ according to (1) and (2) for the desired value R within the transition region. The TES presumably stays in its superconducting state, and the applied RF power (current) cannot produce any Joule heat. Second step is sending to the TES a pulse of Joule heat generated by a resistor. This pulse will switch the device in its normal state. After a some time TES will smoothly relax to lower temperatures following its $R(T)$ curve and eventually reach the heat balance defined by the RF bias power as above. Using this procedure we do not need a precision variable-temperature control. However the *stability* of the bath temperature cannot be neglected along with smooth control over the RF power (0.01 dB step).

To estimate IV-curves of our *wireless devices*, we have to search for self-consistent solutions for RF power P and resistance R across the TES as $P(R(T_{\rm e}(P, T_{\rm bath})))$. The RF power transfer to TES absorber $P(R)$ is calculated using S_{31}-parameter of EM-model, $R(T_{\rm e})$ is obtained from the experiment with the witness bridge (Fig. 6) and $T_{\rm e}(P, T_{\rm bath})$ is based on (5). Each point in Fig. 8 is a self-consistent solution for the various bath temperatures, $T_{\rm bath}$; the voltage, V, is extracted from the incident power, $P_{\rm in}$, in the throughput line. The IV-curves presented in Fig. 8 are very similar to ones reported for the HEB mixers and for the traditional (low-frequency biased) TES bolometers, which are stabilized with the negative electrothermal feedback. Since the matched RF lines are used, the

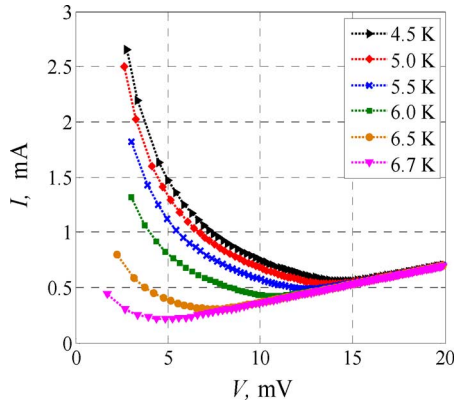

Fig. 8. IV-curves of experimental TES absorber calculated using S-parameters of EM-model. Each point is a self-consistent solution for the dependence $P(R(T_{\rm e}(P, T_{\rm bath})))$ for various bath temperature $T_{\rm bath}$ (see inset) and scanning incident RF power, P, across the absorber. The negative slope of the curves al low voltages is the proof for the voltage source, which is known for providing stability of TES via negative electrothermal feedback.

effect of the excessive inductance at the input of a SQUID is not relevant to the stable operation of the new RF readout.

IV. Conclusion

We have passed successfully the introductory part for development of a new TES detecting device suitable for reaching $\mathrm{NEP} = 10^{-19}$ W/Hz$^{1/2}$ using the convenient RF readout technique, which is similar to the reported MKID readout technique. The new concept is analyzed and compared with existent approaches demonstrating a number of advantageous features, such as low cost, high interference protection and full compatibility with thin-film technology. First experiments with the pilot Nb-devices demonstrate good agreement with EM-modeling. The triggering regime is studied experimentally and a method for initiating the linear regime is suggested via the numerical simulation of dynamics of the device. The margins for the stable operation were found along with presence of the negative electrothermal feedback. We plan a design of a few-pixel array and measurements of its optical sensitivity along with attempts for single-photon detection at μm-wavelength.

References

[1] K. D. Irwin and G. C. Hilton, , Ch. Enss, Ed., "Transition-edge sensors," in *Cryogenic Particle Detection*. Berlin, Germany: Springer-Verlag, 2005, vol. 99, pp. 63–149, Topics Appl. Phys..

[2] S. Ali, L. D. Cooley, D. McCammon, K. L. Nelms, J. Peck, D. Prober, D. Swetz, P. T. Timbie, and D. van der Weide, "Planar antenna-coupled transition-edge hot electron microbolometer," *IEEE Trans. Appl. Supercond.*, vol. 13, no. 2, pt. 1, pp. 184–187, Jun. 2003.

[3] D. F. Santavicca, M. O. Reese, A. B. True, C. A. Schmuttenmaer, and D. E. Prober, "Antenna-coupled niobium bolometers for terahertz spectroscopy," *IEEE Trans. Appl. Supercond.*, vol. 17, no. 3, pt. 1, pp. 412–415, Jun. 2007.

[4] J. Wei, D. Olaya, B. S. Karasik, S. V. Pereverzev, A. V. Sergeev, and M. E. Gershenson, "Ultrasensitive hot-electron nanobolometers for terahertz astrophysics," *Nature Nanotechnol.*, vol. 3, pp. 496–500, 2008.

[5] I. S. McLean, "Instrumentation and detectors," in *Electronic Imaging in Astronomy*, 2nd ed. Chichester, U.K: Springer Praxis, 2008.

[6] J. van der Kuur *et al.*, "The SPICA-SAFARI TES bolometer readout: Developments towards a flight system," *J. Low Temp. Phys.*, vol. 167, no. 5–6, pp. 561–567, 2012.

[7] S. V. Shitov, "Bolometer with high-frequency readout for array applications," *Tech. Phys. Lett.* vol. 37, no. 10, pp. 932–934, 2011 [Online]. Available: http://www.springerlink.com/content/c0j57m70w0m37607/, Transl. *Pis'ma v Zhurnal Tekhnich. Fiziki*, Vol. 37, No. 19, pp. 88–94, 2011

[8] N. Wadefalk, A. Mellberg, I. Angelov, M. E. Barsky, S. Bui, E. Choumas, R. W. Grundbacher, E. L. Kollberg, R. Lai, N. Rorsman, P. Starski , J. Stenarson, D. C. Streit, H. Zirath, and Stenarson, J.; Streit, D.C.; Zirath, H. , "Cryogenic wide-band ultra-low-noise IF amplifiers operating at ultra-low DC power," *IEEE Trans. Microw. Theory Techn.*, vol. 51, no. 6, pp. 1705–1711, 2003.

[9] M.-O. André, M. Mück, J. Clarke, J. Gail, and C. Heiden, "Radiofrequency amplifier with tenth-Kelvin noise temperature based on a microstrip direct current superconducting quantum interference device," *Appl. Phys. Let.*, vol. 75, pp. 698–700, Aug. 1999.

[10] G. V. Prokopenko, S. V. Shitov, I. L. Lapitskaya, V. P. Koshelets, and J. Mygind, "Dynamic characteristics of S-band DC SQUID amplifier," *IEEE Trans. on Appl. Supercond*, vol. 13, no. 2, pp. 1042–1045, June 2003.

[11] P. Day, H. LeDuc, B. Mazin, A. Vayonakis, and J. Zmuidzinas, "A broadband superconducting detector suitable for use in large arrays," *Nature*, vol. 425, pp. 817–821, 2003.

[12] D. F. Filipovic, S. S. Gearhart, and G. M. Rebeiz, "Double-slot antennas on extended hemispherical and elliptical silicon dielectric lenses," *IEEE Trans. Microw. Theory Techn.*, vol. 41, no. 10, pp. 1738–1749, Oct. 1993.

[13] A. F. Andreev, "Thermal conductivity of the intermediate state of superconductors," *Sov. Phys.-JETP*, vol. 19, pp. 1228–1231, 1964.

[14] F. C. Wellstood, C. Urbina, and J. Clarke, "Hot-electron effects in metals," *Phys. Rev. B*, vol. 49, no. 9, pp. 5942–5955, Mar. 1994.

[15] S. I. Park and T. H. Geballe, "$T_{\rm c}$ depression in thin Nb films," *Physica B + C*, vol. 135, no. 1–3, pp. 108–112, 1985.

[16] A. Stockhausen, K. Il'in, M. Siegel, U. Södervall, P. Jedrasik, A. Semenov, and H.-W. Hübers, "Adjustment of self-heating in long superconducting thin film NbN microbridges," *Supercond. Sci. Technol.*, vol. 25, no. 3, p. 035012, 2012.

[17] P. J. Burke, R. J. Schoelkopf, D. E. Prober, A. Skalare, B. S. Karasik, M. C. Gaidis, W. R. McGrath, B. Bumble, and H. G. LeDuc, "Mixing and noise in diffusion and phonon cooled superconducting hot-electron bolometers," *J. Appl. Phys.*, vol. 85, no. 3, pp. 1644–1653, 1999.

[18] E. M. Gershenzon, M. E. Gershenzon, G. N. Gol'tsman, A. M. Lyul'kin, A. D. Semenov, and A. V. Sergeev, "Electron-phonon interaction in ultrathin Nb film," *Sov. Phys. JETP*, vol. 70, no. 3, pp. 505–511, 1990.

[19] R. Schneider, B. Freitag, D. Gerthsen, K. S. Ilin, and M. Siegel, "Structural, microchemical and superconducting properties of ultrathin NbN films on silicon," *Cryst. Res. Technol.*, vol. 44, no. 10, pp. 1115–1121, 2009.

Artyom A. Kuzmin received the Master's degree in applied physics and mathematics from the Moscow Institute of Physics and Technology at department of Problems of Physics and Technology of Nanoelectronics in IMS RAS, Chernogolovka, Russia, in 2007, and the Ph.D. degree from the V.A.Kotelnikov Institute of Radio-engineering and Electronics RAS, Moscow, Russia, in 2011.

His main research area is the development of antenna coupled TES bolometers and HEB mixers and their fabrication techniques.

Sergey S. Shitov received the Diploma degree in physics from the Moscow State University, Moscow, U.S.S.R., in 1982.

His research is oriented on nonlinear superconductor devices for electronic applications: Ph.D thesis (1992) is focused at practicable quantum-noise-limited SIS heterodyne mixers and receiver devices. His Ph.D and Dr.Sci. degrees in physics and mathematics are received from Institute of Radio-engineering and Electronics, Russian Academy of Sciences (IRE RAS), in 1992 and 2003 respectively. From 1992 till 2004, he was a member of Laboratory of Superconducting Devices for Signal Detection and Processing at IRE RAS, developing the Superconducting Integrated Receiver comprising a SIS mixer and a FFO Josephson oscillator along with a SQUID RF amplifier. From 2004 till 2009, he was on leave to the National Astronomical Observatory of Japan developing ALMA Band-10 receiver system. His present research at IRE RAS includes superconducting ultra-low-noise ultra-low-temperature detectors for radio astronomy and superconducting metamaterials at the National University of Science and Technology MISIS. He has authored about 200 technical papers.

Alexander Scheuring received the Diploma degree in electrical engineering and information technologies from the University of Karlsruhe, Germany, in 2007.

In April 2007, he joined the Institute of Micro- and Nanoelectronic systems, University of Karlsruhe (later Karlsruhe Institute of Technology). He works on the design and development of quasi-optical receiver concepts for superconducting THz radiation detectors. From February 2008 to July 2008, he was with the LGEP-Supelec in Paris, France, where he was involved in the development of ultra-wideband high-impedance antennas for semiconducting room-temperature THz bolometers.

Johannes Maximilian Meckbach (GSM'11) received the Diploma degree in electrical engineering and information technologies from the Karlsruhe Institute of Technology, Germany, in 2009. In June 2009, he joined the Institute of Micro- and Nanoelectronic Systems, Karlsruhe Institute of Technology, Karlsruhe, Germany. His main research area is the development of Josephson junctions (JJs) and fabrication techniques thereof. Besides investigation of fundamental vortex physics in long JJs, he is also involved in SQUID development and development of integrated THz receivers.

Konstantin S. Il'in was born in Moscow, U.S.S.R. on March 24, 1968. He received the Ph.D. degree in solid-state physics from Moscow State Pedagogical University (MSPU), Moscow, Russia, in 1998.

From 1997 to 1998, he was a Visiting Scientist with the Electrical and Computer Engineering Department, University of Massachusetts at Amherst, and with the Electrical Engineering Department, University of Rochester, Rochester, NY. From January 1998 to June 1999, he was an Assistant Professor with the Physics Department, MSPU. From 1999 to 2003, he was a Scientific Researcher with the Institute of Thin Films and Interfaces, Research Center Juelich, Juelich, Germany. In June 2003, he joined the Institute of Micro- and Nano-electronic Systems, University of Karlsruhe, Karlsruhe, Germany, where he currently develops technology of ultrathin films of conventional superconductors for receivers of electromagnetic radiation. His research interests include fabrication and study of normal state and superconducting properties of submicrometer- and nanometer-sized structures from ultrathin films of disordered superconductors.

Stefan Wuensch received the Dipl.-Ing. and the Dr.-Ing. degrees in electrical engineering from the University of Karlsruhe, Karlsruhe, Germany, in 1998 and 2005, respectively.

In November 1998, he joined the Institut für Elektrotechnische Grundlagen der Informatik, University of Karlsruhe. Since September 2002, he joined the Institut für Mikro- und Nanoelektronische Systeme, University of Karlsruhe. His main research interest are passive microwave devices for detector applications and cryogenic microwave amplifiers for detector readout systems.

Alexey V. Ustinov received the Diploma degree in physics from Moscow University of Physics and Technology and the Ph.D. degree in solid state physics from the Institute of Solid State Physics in Chernogolovka, USSR, in 1984 and 1987, respectively.

In 1989, he received the Alexander von Humboldt Fellowship and worked for two years at the University of Tuebingen in Germany. His research was focused on fluxon dynamics in long Josephson junctions and thermoelectric effects in high-temperature superconductors. In 1991–1993 he stayed for long-term visits at the Technical University of Denmark and the University of Rome "Tor Vergata", Italy. In 1993, he joined the Institute for Thin Film and Ion Technology at Research Center Juelich in Germany. There he worked on Josephson stacks and mm-wave oscillators. In 1996, he accepted an associate professor position at the University of Erlangen-Nuremberg in Germany and worked on superconducting circuits and qubits. In 2008, he moved as full professor of physics to the University of Karlsruhe, Germany (presently the Karlsruhe Institute of Technology), where his research includes superconducting qubits and metamaterials, microwave experiments with quantum circuits, and hybrid quantum devices. He has authored over 250 technical papers.

Michael Siegel received the Diploma degree in physics and the Ph.D. degree in solid state physics from the Moscow State University, Moscow, U.S.S.R., in 1978 and 1981, respectively.

In 1981, he joined the University of Jena where he held positions as Staff Member and later as Group Leader in the Superconductive Electronic Sensor Department. His research was oriented on nonlinear superconductor-semiconductor devices for electronic applications. In 1987, he initiated research at the University of Jena in thin-film high temperature superconductivity (HTS) for Josephson junction devices, mainly for SQUID. In 1991, he left to join the Institute for Thin Film and Ion Technology at Research Center Juelich. There he worked on development and application of HTS Josephson junctions, SQUID, microwave arrays and mixers, and high-speed digital circuits based on rapid single- flux-quantum logic. In 2002, he received a Full Professor position at University of Karlsruhe, Germany, where he is now the Director of the Institute of Micro- and Nanoelectronic Systems. His research includes transport phenomena in superconducting, quantum and spin dependent tunneling devices. He has authored over 200 technical papers.